Neuroglobin-overexpressing transgenic mice are resistant to cerebral and myocardial ischemia

Adil A. Khan, Yaoming Wang, Yunjuan Sun, Xiao Ou Mao, Lin Xie, Erin Miles, Justin Graboski, Sylvia Chen, Lisa M. Ellerby, Kunlin Jin, and David A. Greenberg*

Buck Institute for Age Research, Novato, CA 94945

Edited by Solomon H. Snyder, Johns Hopkins University School of Medicine, Baltimore, MD, and approved October 3, 2006 (received for review August 28, 2006)

Neuroglobin (Ngb), a protein related to myoglobin and hemoglobin but expressed predominantly in the brain, is induced by neuronal hypoxia and cerebral ischemia and protects against hypoxic or ischemic neuronal injury. We engineered transgenic mice that overexpress murine Ngb under the control of a chicken β-actin promoter, resulting in enhanced Ngb expression in multiple cell types and multiple tissues, including brain and heart. In Ngb-overexpressing transgenic mice compared with wild-type littermates, the volume of cerebral infarcts after occlusion of the middle cerebral artery was reduced by ≈30%, and the volume of myocardial infarcts produced by occlusion of the left anterior descending coronary artery was reduced by ≈25%. Ngb overexpression was associated with enhanced expression of endothelial nitric oxide synthase in vascular endothelial cells. These findings extend prior evidence for cytoprotection by Ngb and suggest both direct (parenchymatous) and indirect (vasomotor) protective mechanisms.

endothelial nitric oxide synthase | myocardial infarction | stroke

Neuroglobin (Ngb) is a monomeric globin expressed in neurons and some endocrine cells of vertebrates, including humans (1). Ngb shows ≈20% amino acid homology to myoglobin (Mb) and Hb, and ≈30% homology to an intracellular nerve globin found in the annelid *Aphrodite aculeata* (2). Like Mb and Hb, Ngb binds O_2 with high affinity, suggesting a possible role in O_2 storage, transport, or sensing (1, 3–5). The association of retinal Ngb with sites rich in mitochondria and high in O_2 demand is consistent with such functions (6). Another possibility is that Ngb is involved in signaling or toxicity associated with nitric oxide (NO) or carbon monoxide (CO), with which it also forms complexes (4, 7). Finally, Ngb acts as a guanine nucleotide dissociation inhibitor (8) and interacts with neuronal membrane proteins, including Na^+, K^+-ATPase (9), and flotillin-1 (10). However, the relative importance of these actions and the physiological cellular functions they subserve *in vivo* are unclear.

Mb and Hb are induced by hypoxia, such as occurs at high altitudes (11, 12). In hypoxia-tolerant fish, Mb is also expressed ectopically in tissues like liver, gills, and brain (13). Moreover, forced overexpression of Mb confers production from ischemia–reperfusion injury in rat liver (14). Thus, there is precedent for hypoxic induction of globins and for globin-mediated cytoprotection in nonneural tissues. Accordingly, the O_2-binding capacity and predominantly neuronal localization of Ngb led us to investigate its neuroprotective potential. In primary neuronal cultures, Ngb mRNA and protein expression was increased by hypoxia and by the hypoxia simulators, cobalt and deferoxamine (15). Antisense inhibition of Ngb expression increased neuronal susceptibility to hypoxic death, whereas forced overexpression of Ngb with a plasmid vector conferred hypoxia resistance. In studies on rats subjected to focal cerebral ischemia induced by middle cerebral artery (MCA) occlusion (16), intraventricular administration of a Ngb antisense oligonucleotide increased infarct volume and associated neurological deficits, whereas a Ngb-expressing adeno-associated vector, delivered intracerebrally, reduced infarct size and neurological impairment. Additional reports of hypoxic or ischemic induction of neuronal Ngb expression have been published (17–19). Taken together, these findings are consistent with a protective role of Ngb against hypoxic and ischemic injury.

To investigate further the cytoprotective action of Ngb, we generated transgenic mice that overexpress Ngb in multiple body tissues. Here we report that Ngb transgenic (Ngb-Tg) mice show reduced sensitivity to ischemia both in brain, where Ngb is normally expressed, and in heart, where it is not.

Results

Transgenic Mice. Ngb-Tg mice showed no perinatal lethality and appeared and behaved normally up to at least 6 months of age. Constitutive Ngb protein expression was increased in brain and heart of Ngb-Tg compared with wild-type mice (Fig. 1), as well as in other tissues. In cerebral cortex, Ngb-Tg mice showed increased numbers of neurons (Fig. 2*a*), astrocytes (Fig. 2*b*), and endothelial cells (not shown) that constitutively expressed Ngb. Ngb was also constitutively expressed in Ngb-Tg mouse heart (Fig. 2*c*), where it was associated most prominently with vascular endothelial cells (Fig. 2*d*).

Focal Cerebral Ischemia. In both wild-type and Ngb-Tg mice, MCA occlusion produced an ipsilateral infarct affecting primarily the striatum and cerebral cortex (Fig. 3a). In Ngb-Tg mice, however, infarct volume was ≈30% smaller (Fig. 3 a and b). A similar reduction was observed whether infarct volume was measured by 2,3,5-triphenyltetrazolium hydrochloride (TTC) or cresyl violet staining. Histological sections through the area of infarction showed pyknotic nuclei and perineuronal vacuolation consistent with ischemic injury (Fig. 3c). Pre-, intra-, and postischemic regional cerebral blood flow was similar in wild-type and Ngb-Tg mice (Fig. 3d), indicating that changes in blood flow are unlikely to explain the protective effect of Ngb overexpression in focal cerebral ischemia.

Myocardial Ischemia. Occlusion of the left anterior descending coronary artery (LADA) produced a transmural infarct affecting the left ventricle (Fig. 4 a and b). Histological sections through ischemic myocardium showed narrow wavy muscle fibers with pyknotic nuclei and interstitial edema (Fig. 4c). Infarct size,

Author contributions: A.A.K., L.M.E., K.J., and D.A.G. designed research; A.A.K., Y.W., Y.S., X.O.M., L.X., E.M., J.G., S.C., and K.J. performed research; Y.W. and Y.S. contributed new reagents/analytic tools; A.A.K., Y.W., L.M.E., K.J., and D.A.G. analyzed data; and D.A.G. wrote the paper.

The authors declare no conflict of interest.

This article is a PNAS direct submission.

Abbreviations: Mb, myoglobin; MCA, middle cerebral artery; Ngb-Tg, Ngb transgenic; TTC, 2,3,5-triphenyltetrazolium hydrochloride; LADA, left anterior descending coronary artery; NO, nitric oxide; eNOS, endothelial NO synthase.

*To whom correspondence should be addressed. E-mail: dgreenberg@buckinstitute.org.

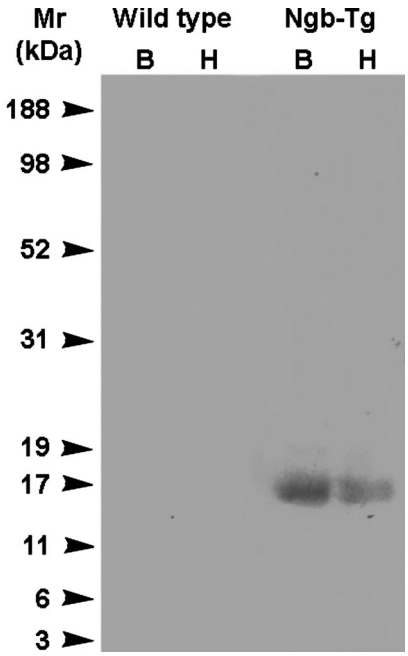

Fig. 1. Western blot analysis of constitutive Ngb expression in brain (B) and heart (H) of wild-type and Ngb-Tg mice.

expressed as a percentage of either left ventricular volume or as a percentage of the LADA territory (area at risk), was ≈25% smaller in Ngb-Tg mice. In contrast, there was no difference between wild-type and Ngb-Tg mice in area at risk as a percentage of left ventricular volume, indicating that the observed changes in infarct size could not be attributed to differences in the extent of the LADA territory in Ngb-Tg mice.

To begin to explore how Ngb, which is not normally expressed in the heart, might provide cardioprotection in Ngb-Tg mice, we considered its predominantly endothelial localization in myocardial tissue. One well documented endothelium-based mechanism for protection against both cerebral (20) and myocardial (21, 22) ischemia is the production of NO by endothelial NO synthase (eNOS). Staining of myocardial sections from Ngb-Tg mice with an antibody against eNOS revealed markedly increased eNOS immunoreactivity, compared with myocardium from wild-type mice (Fig. 4d), and increased eNOS expression was also detected on Western blots (Fig. 4e), suggesting that up-regulation of eNOS might contribute to Ngb-induced cardioprotection.

Discussion

The main finding we report is that mice engineered to constitutively overexpress Ngb show reductions in infarct size after both cerebral and myocardial ischemia. Ngb-Tg mice displayed no overt phenotypic abnormalities. Ngb was constitutively overexpressed in multiple cell types, including both neurons and astrocytes in brain, and in multiple organs, including heart. As found in rats given intracerebral injections of a Ngb-expressing adeno-associated vector (16), Ngb-Tg mice had substantially smaller cerebral infarcts after MCA occlusion, compared with wild-type littermates. Although Ngb is not normally expressed in the heart (1), its transgenic overexpression in the present study

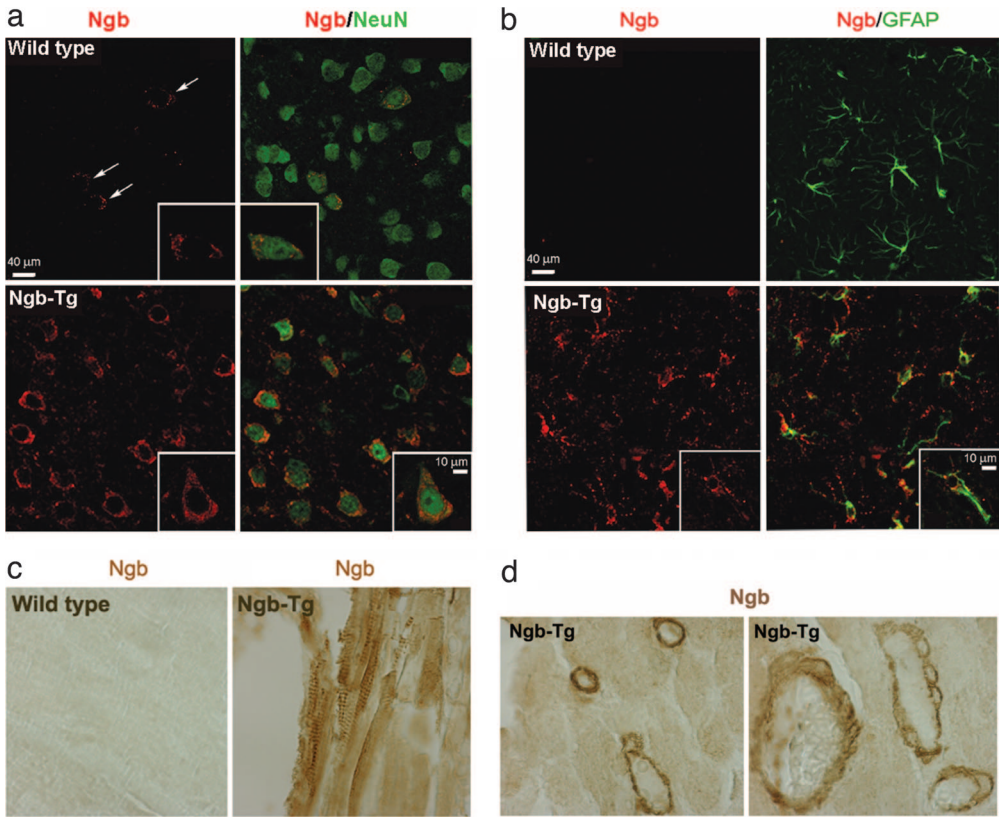

Fig. 2. Immunohistochemical localization of Ngb expression in relation to expression of the neuronal marker NeuN (a) and the astroglial marker GFAP (b) in mouse cerebral cortex, and in muscle (c) and vascular endothelium (d) from mouse heart. Arrows in a show NeuN-immunopositive cells expressing low constitutive levels of Ngb in brain. *Insets* (a and b) and d Right show examples of Ngb-immunopositive cells at higher magnification.

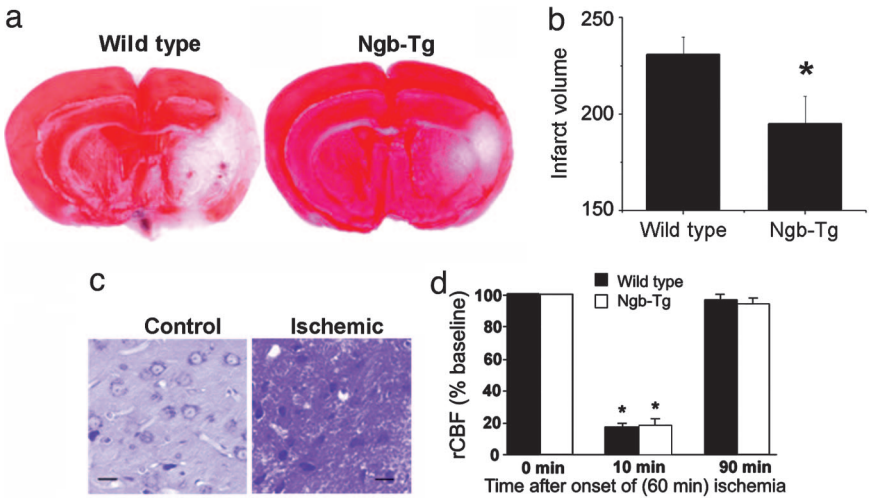

Fig. 3. Effect of transgenic overexpression of Ngb on the size of cerebral infarcts produced by MCA occlusion. (a) Representative TTC-stained sections showing viable, stained (red), and ischemic, unstained (white) brain tissue. (b) Mean infarct volumes ± SEM (n = 5); *, $P < 0.001$ compared with wild type. (c) Cresyl violet-stained sections from nonischemic control (Left) and ischemic (Right) regions of Ngb-overexpressing transgenic mouse brain corresponding to TTC-stained and unstained areas, respectively. (d) Regional cerebral blood flow measured by laser-Doppler flowmetry before (0 min), during (10 min) and after (90 min) 60 min of cerebral ischemia in wild-type and Ngb-overexpressing transgenic mice. *, $P < 0.05$ compared with 0 and 90 min, but no difference between wild type and Ngb-Tg.

also afforded partial protection against myocardial infarction from disruption of blood flow in the LADA.

Ngb binds O_2 with high affinity, and early reports pointed to a likely role in O_2 transport (1). Support for such a function includes the observations that Ngb protects cultured neuronal cells from hypoxia (15), and that Ngb expression in the retina parallels metabolic activity (23), although O_2 consumption is not increased in Ngb-transfected cells (15). Like Mb and Hb, Ngb also binds other gaseous messengers, including NO and CO (4, 7), which are important in signal transduction (24). Nevertheless, Ngb-transfected cells were no less sensitive than control cells to the cytotoxicity of the NO-releasing drug sodium nitroprusside (15). Wakasugi *et al.* (8) proposed a novel role for Ngb as a sensor of oxidative stress in brain, based on its homology to regulators of G protein signaling (RGS) and RGS domains of G protein-coupled receptor kinases. They found that oxidation of ferrous to ferric iron in Ngb conferred guanine nucleotide dissociation inhibitor activity, whereby Ngb inhibits the exchange

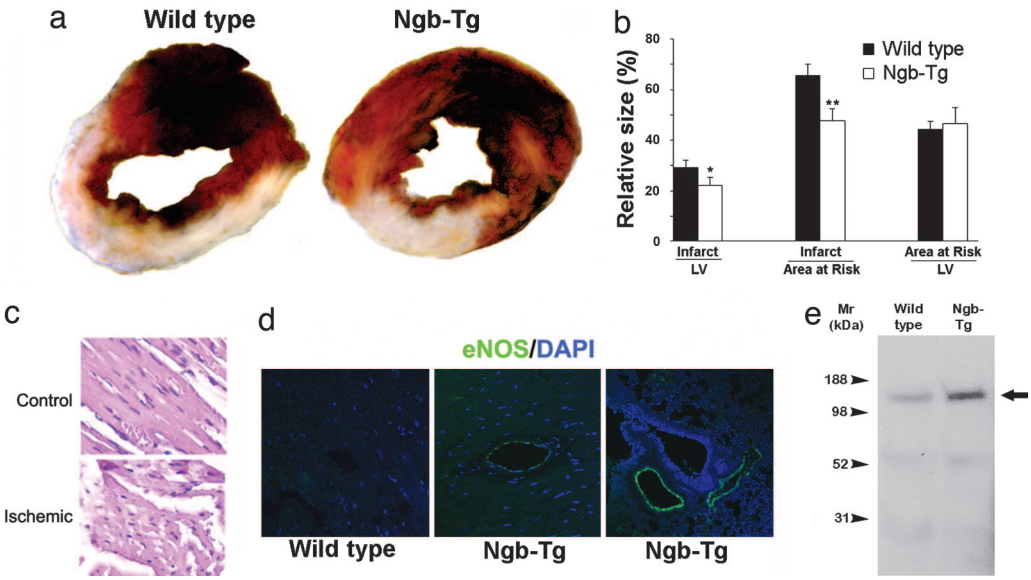

Fig. 4. Effect of transgenic overexpression of Ngb on the size of myocardial infarcts produced by LADA occlusion. (*a*) Representative TTC-stained sections showing viable (red) and ischemic (white) heart tissue. Evans blue dye (blue) delineates tissue outside the territory of the LADA and, therefore, not at risk for infarction from LADA occlusion. (*b*) Mean infarct volumes ± SEM, expressed as a percentage of left ventricular (LV) volume and of LV volume at risk from LADA occlusion, and volume at risk as a percentage of total LV volume ($n = 5$); *, $P < 0.01$; **, $P < 0.001$ compared with wild type. (*c*) H&E-stained sections from nonischemic control (*Left*) and ischemic (*Right*) regions of Ngb-overexpressing transgenic mouse heart corresponding to TTC-stained (red) and unstained (white) areas, respectively. (*d*) eNOS immunoreactivity (green) in myocardium of wild-type (*Left*) and myocardium (*Center*), and lung (*Right*) of Ngb-overexpressing transgenic mice, showing predominant localization to vascular endothelium. Nuclei (blue) are counterstained with DAPI. (*e*) Western blot of eNOS expression (right arrow) in heart of wild-type and Ngb-overexpressing transgenic (Ngb-Tg) mice.

of GDP for GTP by $G\alpha_i$. As a result, they argued, ferrous Ngb would liberate free $G_{\beta\gamma}$, activating signaling pathways that promote cell survival (25).

Notwithstanding that the specific mechanism for Ngb-mediated neuroprotection from hypoxia or ischemia is unclear, two observations suggest that a direct effect on neurons is involved. First, Ngb is an intracellular protein expressed almost exclusively in neurons *in vivo* (1). Second, Ngb is protective in primary neuronal cultures and cultured neural cell lines, where other cell types are absent (15). How overexpression of Ngb might protect the heart from ischemia is less obvious. However, the observation that overexpression of Ngb reduces ischemic injury to myocardial cells, which contain vastly greater amounts of Mb (26), makes it likely that Ngb operates by a unique mechanism not shared by Mb. The increased expression of endothelial cell eNOS observed in the hearts of Ngb-overexpressing mice is of interest, because mice engineered to overexpress eNOS in vascular endothelial cells show reduced infarct size after transient myocardial ischemia (22), whereas eNOS-knockout mice have larger infarcts (21). It is, therefore, possible that the protective effect of Ngb overexpression against myocardial ischemia is mediated through enhanced expression of eNOS. Because eNOS also has a protective role against cerebral ischemia (20), a similar mechanism could contribute to the observed reduction in cerebral infarct volume after MCA occlusion. Such an effect might synergize with the direct neuroprotective effect of Ngb observed, for example, during hypoxia *in vitro* (15).

The ability of a transgenically expressed intracellular protein like Ngb to reduce ischemic injury does not translate obviously into a therapeutic strategy. However, we found previously that intracerebral administration of Ngb by an adeno-associated vector reduced the size of cerebral infarcts (16). Moreover, some pathways involved in the induction of Ngb expression have been identified and might represent targets for small-molecule drugs. Hypoxic induction of Ngb appears to depend on MAPK, because it is blocked by the MAPK/extracellular signal-regulated kinase kinase inhibitor, PD98059 (27). Induction of Ngb expression by hemin involves protein kinase G and soluble guanylate cyclase, because it is inhibited by KT5832 and LY83583, respectively, and stimulated by 8-bromo-cGMP (27). Consequently, drugs that target these pathways might afford protection from ischemia by up-regulating Ngb levels in brain or other tissues at risk.

Materials and Methods

Transgenic Animals. All animal experiments were approved by the Buck Institute's Animal Care and Use Committee and conducted according to National Institutes of Health guidelines. A full-length cDNA fragment of mouse Ngb, kindly provided by Thomas Hankeln (Institute of Molecular Genetics, University of Mainz, Mainz, Germany), was subcloned into the SpeI and EcoRV restriction sites of the pTR-UF12d vector, upstream of the chicken β-actin promoter and the distal CMV enhancer, and downstream of GFP, to generate a Ngb-GFP vector. All final plasmids were verified by sequencing and overexpression of Ngb and GFP proteins in the 293 cell line and confirmed by Western blot. Plasmids were digested with restriction enzymes to remove bacterial sequences, purified using QIAEX II Gel extraction kits (Qiagen, Valencia, CA), and microinjected into fertilized eggs of BDF $\times$ CD1 mice, as described (28). Mouse tail DNA was screened by PCR for the presence of the transgenes. We generated five BDF $\times$ CD1 founder mice that expressed the GFP transgene, three of which showed increased expression of Ngb in brain by RT-PCR and Western blotting. Crosses between heterozygous Ngb-Tg mice yielded offspring in the expected Mendelian ratio of 1:2:1, as determined by genotyping at 7–10 days of age. Homozygous Ngb-Tg mice were compared with wild-type littermates in all experiments. For genotyping, mouse tail DNA was screened by PCR by using specific primers (5′-GGGTTACTCCCACAGGTGAG-3′ and 5′-CAAGCTGGTCAGGTACTCCTCC-3′ for Ngb 506-bp product; 5′-GCGGTCACAAACTCCAGCAGGACCA-3′ and 5′-GGCGTGGTCCCAATCTCGTGGAA-3′ for GFP 664-bp product). Ngb-Tg mice used in this study were offspring of intersibling matings over at least six generations.

RT-PCR. Mouse total RNA was isolated from different brain regions by using the RNeasy Mini kit (Qiagen), and reverse-transcribed into first-strand cDNA using the Reverse Transcription System and Oligo dT_{12-18}, according to the manufacturer's instructions. After RT, samples equivalent to 2 ng of RNA were mixed in a 25-μl reaction mixture containing 20 mM Tris·HCl (pH. 8.4), 50 mM KCl, 2 mM $MgCl_2$, 0.5 mM dNTPs, 1 unit Taq polymerase, and 0.5 nM each of Ngb or GFP primers as described above. PCR amplification was performed by using the following conditions: 94°C for 5 min, followed by 30 cycles of 94°C for 30 s, 57°C for 30 s, 72°C for 45 s, and 72°C for 5 min. PCR products were analyzed by electrophoresis on 1% agarose gels.

Western Blotting. Cell lysates were extracted in PBS containing 1% Nonidet P-40, 0.5% sodium deoxycholate, 0.1% SDS, 1 μg/ml aprotinin, and 100 μg/ml phenylmethylsulfonyl fluoride, and protein concentration was determined by using a Bio-Rad (Hercules, CA) protein assay. Protein (50 μg per sample) was boiled at 100°C in SDS sample buffer for 5 min, electrophoresed on 12% SDS/PAGE gels, and transferred to polyvinyldifluoridine membranes. These were then incubated with affinity-purified goat anti-Ngb (1:200; Santa Cruz Biotechnology, Santa Cruz, CA) or rabbit polyclonal anti-eNOS (1:200; Santa Cruz Biotechnology). Membranes were washed with PBS containing 0.1% Tween-20, incubated with horseradish peroxidase-conjugated anti-mouse or -goat secondary antibody (Santa Cruz Biotechnology; 1:3,000) at room temperature for 60 min, and washed three times for 15 min with PBS/Tween-20. Peroxidase activity was visualized with a chemiluminescence substrate system (NEN Life Science, Boston, MA).

Fluorescence Immunohistochemistry. Fluorescence immunohistochemistry was performed as described (15, 16). The primary antibodies were goat polyclonal anti-Ngb (1:200; Santa Cruz Biotechnology), mouse monoclonal anti-NeuN (1:200; Chemicon, Hampshire, U.K.), mouse monoclonal anti-GFAP (1:150; Sigma, St. Louis, MO), and rabbit polyclonal anti-eNOS (1:200; Santa Cruz Biotechnology). The secondary antibodies were FITC-conjugated rat-absorbed donkey anti-mouse, rhodamine-conjugated donkey anti-goat, and Alexa Fluor 488 donkey anti-rabbit IgG (Jackson ImmunoResearch, West Grove, PA; 1:200). Fluorescence signals were detected with a Nikon (Florham Park, NJ) E800 microscope at excitation/emission wavelengths of 535/565 nm (rhodamine, red), 470/505 (FITC, green) and 360/400 (DAPI, blue). Results were recorded with a Magnifire digital camera (ChipCoolers, Warwick, RI). Controls included omitting or preabsorbing primary and omitting secondary antibody. Selected images were viewed at high magnification by using a Nikon PCM-2000 laser-scanning confocal microscope and Simple PCI imaging software (Compix, Cranberry Township, PA).

Focal Cerebral Ischemia. As described (29), male mice (30–35 gm) were anesthetized with 1.5% isoflurane in 70% N_2O/30% O_2. Rectal temperature was maintained at 37.0 $\pm$ 0.5°C with a thermostat-controlled heating blanket. The left external carotid artery was ligated with 6–0 silk suture, and its branches were electrocoagulated. An 8–0 silicon-coated monofilament surgical nylon suture with a heat-blunted tip was introduced into the left

internal carotid artery through the stump of the external carotid and advanced 12 mm past the common carotid artery bifurcation to occlude the left MCA. The left common carotid artery was also occluded during the period of MCA occlusion. The filament was sutured in place for 60 min and then withdrawn. Regional cerebral blood flow was measured by laser-Doppler flowmetry with a probe placed through a burr hole drilled 1.5 mm lateral to the midline and 1.7 mm anterior to the lambda. Mice were killed after 24 h of reperfusion, and brains were removed for histological analysis. Brain infarct area was measured on 2-mm coronal brain sections, which were immersed in 2% TTC in PBS for 20 min at 37°C and then fixed overnight at 4°C in 4% paraformaldehyde (30). Infarct volume was calculated by integrating the infarction areas, corrected for edema (29).

Myocardial Ischemia. Myocardial ischemia was induced as described in ref. 31. Mice were given gentamicin (0.7 mg/kg i.m.), premedicated with atropine sulfate (0.04 mg/kg i.m.), and anesthetized with sodium pentobarbital (50 mg/kg i.p. followed by additional doses as required to maintain anesthesia). They were intubated and ventilated at a tidal volume of 2.1–2.5 ml and a rate of 105 min^{-1}. A catheter was placed in the external jugular vein to provide fluids and, in some cases, in the carotid artery to measure blood pressure and blood gases. Body temperature was monitored with a rectal probe and maintained at 37.0°C with a heating pad and lamp. Approximately 0.4 ml of blood was given before thoracotomy, immediately after thoracotomy, and after the chest was closed, to maintain mean arterial blood pressure ≥80 mm of Hg. The chest was opened through a midline sternotomy and 8–0 nylon suture was passed under the LADA, 2–3 mm from the tip of the left auricle. A nontraumatic balloon occluder was applied and inflated to occlude the artery, and occlusion was verified by myocardial pallor. The chest was closed, and mice were extubated, removed from the ventilator, provided with fluids (1.0–1.5 ml of 5% dextrose i.p.) and 100% O_2 by nose cone, and kept warm with a heating lamp. Twenty-four hours later, mice were given heparin (1 unit/g i.p.), anesthetized with sodium pentobarbital (35 mg/kg i.p.), and killed with an i.v. bolus of KCl. The aorta was cannulated with a 22-gauge Luer stub, and 1% Evans blue was perfused into the aorta and coronary arteries to stain the ventricular wall proximal to the coronary artery ligature. The heart was excised and the left ventricle was divided into six transverse slices, which were incubated with 1% TTC in phosphate buffer (pH 7.4, 37°C) to identify viable tissue (31). The slices were photographed and infarct size was calculated by using the NIH Image program.

Statistical Analysis. Data were analyzed by Student's t test for single comparisons and by ANOVA and post-hoc Student—Newman–Keuls tests for multiple comparisons. $P < 0.05$ was considered statistically significant.

This work was supported by National Institutes of Health Grant NS35965 (to D.A.G.).

1. Burmester T, Weich B, Reinhardt S, Hankeln T (2000) *Nature* 407:520–523.
2. Dewilde S, Blaxter M, Van Hauwaert ML, Vanfleteren J, Esmans EL, Marden M, Griffon N, Moens L (1996) *J Biol Chem* 271:19865–19870.
3. Couture M, Burmester T, Hankeln T, Rousseau DL (2001) *J Biol Chem* 276:36377–36382.
4. Dewilde S, Kiger L, Burmester T, Hankeln T, Baudin-Creuza V, Aerts T, Marden MC, Caubergs R, Moens L (2001) *J Biol Chem* 276:38949–38955.
5. Trent JT, 3rd, Watts RA, Hargrove MS (2001) *J Biol Chem* 276:30106–30110.
6. Schmidt M, Giessl A, Laufs T, Hankeln T, Wolfrum U, Burmester T (2003) *J Biol Chem* 278:1932–1935.
7. Van Doorslaer S, Dewilde S, Kiger L, Nistor SV, Goovaerts E, Marden MC, Moens L (2003) *J Biol Chem* 278:4919–4925.
8. Wakasugi K, Nakano T, Morishima I (2003) *J Biol Chem* 278:36505–36512.
9. Xu WL, Wang CL, Liao ZY, Zhang YL, Yu LH, Meng FW, Wang XX, Yin ZY, Qian LJ, Zhang CG (2003) *Acta Biochim Biophys Sin (Shanghai)* (2003) 35:823–828.
10. Wakasugi K, Nakano T, Kitatsuji C, Morishima I (2004) *Biochem Biophys Res Commun* 318:453–460.
11. Reynafarje B (1962) *J Appl Physiol* 17:301–305.
12. Hoppeler H, Vogt M (2001) *J Exp Biol* 204:3133–3139.
13. Fraser J, Vieira de Mello L, Ward D, Rees HH, Williams DR, Fang Y, Brass A, Gracey AY, Cossins AR (2006) *Proc Natl Acad Sci USA* 103:2977–2981.
14. Nitta T, Xundi X, Hatano E, Yamamoto N, Uehara T, Yoshida M, Harada N, Honda K, Tanaka A, Sosnowski D, *et al.* (2003) *J Surg Res* 110:322–331.
15. Sun Y, Jin K, Mao XO, Zhu Y, Greenberg DA (2001) *Proc Natl Acad Sci USA* 98:15306–15311.
16. Sun Y, Jin K, Mao XO, Zhu Y, Greenberg DA (2003) *Proc Natl Acad Sci USA* 100:3497–3500.
17. Li RC, Lee SK, Pouranfar F, Brittian KR, Clair HB, Row BW, Wang Y, Gozal D (2006) *Brain Res* 1096:173–179.
18. Schmidt-Kastner R, Haberkamp M, Schmitz C, Hankeln T, Burmester T (2006) *Brain Res* 1103:173–180.
19. Shang A, Zhou D, Wang L, Gao Y, Fan M, Wang X, Zhou R, Zhang C (2006) *Brain Res* 1078:219–226.
20. Huang Z, Huang PL, Ma J, Meng W, Ayata C, Fishman MC, Moskowitz MA (1996) *J Cereb Blood Flow Metab* 16:981–987.
21. Jones SP, Girod WG, Palazzo AJ, Granger DN, Grisham MB, Jourd'Heuil D, Huang PL, Lefer DJ (1999) *Am J Physiol* 276:H1567–H1573.
22. Jones SP, Greer JJ, Kakkar AK, Ware PD, Turnage RH, Hicks M, van Haperen R, de Crom R, Kawashima S, Yokoyama M, *et al.* (2004) *Am J Physiol* 286:H276–H282.
23. Schmidt M, Giessl A, Laufs T, Hankeln T, Wolfrum U, Burmester T (2002) *J Biol Chem* 278:1932–1935.
24. Baranano DE, Ferris CD, Snyder SH (2001) *Trends Neurosci* 24:99–106.
25. Schwindinger WF, Robishaw JD (2001) *Oncogene* 20:1653–1660.
26. Brunori M, Giuffre A, Nienhaus K, Nienhaus GU, Scandurra FM, Vallone B (2005) *Proc Natl Acad Sci USA* 102:8483–8488.
27. Zhu Y, Sun Y, Jin K, Greenberg DA (2002) *Blood* 100:2494–2498.
28. Hogan BL, Costantini F, Lacy E (1986) *Manipulating the Mouse Embryo: A Laboratory Manual* (Cold Spring Harbor Laboratory Press, Cold Spring Harbor, NY).
29. Parmentier-Batteur S, Jin K, Mao XO, Xie L, Greenberg DA (2002) *J Neurosci* 22:9771–9775.
30. Bederson JB, Pitts LH, Germano IM, Nishimura MC, Davis RL, Bartkowski HM (1986) *Stroke* 17:1304–1307.
31. Guo Y, Wu WJ, Qiu Y, Tang XL, Yang Z, Bolli R (1998) *Am J Physiol* 275:H1375–H1387.